

Numerical Investigation of Shock-Induced Combustion around a Cylindrical Body

Taku Segawa and Akiko Matsuo

Keio University, Hiyoshi 3-14-1, Kohoku-ku, Yokohama, Kanagawa, Japan

1 Introduction

Shock-induced combustion around a spherical projectile flying at hypervelocity into a combustible gas was investigated in a number of ballistic range experiments in the 1960s and 1970s. Lehr performed one of the most famous experiments in 1972 [1]. He caught the unsteady shock-induced combustion on shadowgraph pictures at the specific conditions, in which periodic oscillation of reaction front is clearly observed. The oscillation pattern of unsteady shock-induced combustion is classified into two regimes, the regular regime and the large-disturbance regime, depending on the manner of the oscillation. The regular regime, which was observed in Lehr's experiment, has a high-frequency oscillation, and the reaction front and the bow shock wave are always detached. On the other hand, the large-disturbance regime has a low-frequency oscillation, and the reaction front penetrates the bow shock wave periodically. The unsteady state, whose unsteadiness is stronger than the previous two regimes and whose oscillation is not periodic because of the transverse wave propagating toward the stagnation streamline, was also observed.

Shock-induced combustion around spherical projectiles has also been investigated by numerical simulation. Matsuo and Fujii [2] carried out the two-dimensional simulation under the axisymmetric assumption for both the regular regime and the large-disturbance regime, and clarified the mechanisms of them.

SHCRAMJET (SHock-induced Combustion RAMJET) engine is one of the applications of shock-induced combustion. It is difficult to fix a spherical body on a combustor of such engines. We can say that a cylindrical body is more suitable for a body inducing shock-induced combustion than a spherical one because a cylinder can be held on a combustor by supporting both ends. However, there are few investigations of shock-induced combustion around cylindrical bodies. So the aim of this work is to clarify the flow field of shock-induced combustion around cylindrical bodies using two- and three-dimensional numerical analysis.

2 Numerical Setup

The governing equations are the compressible and reactive two- and three-dimensional Euler equations. The two-step chemical reaction model proposed by Korobeinikov et al. [3] is used to reduce the computational load. This simplified model represents the reaction mechanism with two phases, the induction and exothermic period, based on the ZND model. The parameters of this model in the present work are the same as those of Matsuo and Fujii [2]. The pre-exponential factors of the first and second reactions are $k_1 = 3.0 \times 10^8 \text{ m}^3/(\text{kg} \cdot \text{s})$ and $k_2 = 2.74 \times 10^{-5} \text{ m}^4/(\text{N}^2 \cdot \text{s})$, respectively. The activation energies and the heat releases are $E_1/R = 10000\text{K}$, $E_2/R = 3400\text{K}$ and $Q = 2.2 \times 10^6 \text{ J/kg}$, respectively. For the discretization of convective term and the method of time integration, Yee's Non-MUSCL Type

2nd-Order Upwind TVD Scheme and point-implicit method, which treats only source term implicitly, are used respectively. We used one of Lehr's gas conditions [1] for cylindrical bodies of 3mm diameter in two- and three-dimensional computational space: the hypervelocity stoichiometric hydrogen-air mixture at 1931m/sec under the initial pressure $p_0 = 0.421$ atm, the temperature $T_0 = 293$ K and the specific heat ratio $\gamma=1.4$. Figure 1 shows the computational domain used in three-dimensional analysis. 13 grid points in the induction length are set in η direction where the transverse detonation propagates. The periodic condition is used for the boundary condition of spanwise direction (red zone) and the mirror condition for the vertical symmetry plane (yellow zone). The diameter is constant with 3mm. We used the result of two-dimensional analysis for the initial condition of three-dimensional one, with the initial disturbance, whose conditions are the same as those of the incoming flow, behind the shock wave to induce the axial flow.

3 Results and Discussions

Figure 2 shows the density contour plots of (a) the regular regime, (b) the large-disturbance regime and (c) the unsteady state around cylindrical bodies of 3, 7, 8mm diameter in two-dimensional analysis. These flow regimes follows the same mechanisms as observed around spherical bodies in both experiments and numerical analyses in the past. When the diameter d is 3mm, the regular regime is observed in two-dimensional analysis, but in three-dimensional analysis the transverse detonation is observed in front of cylindrical body. Figure 3 shows the time evolution of the isosurfaces of the reaction fronts for $L=5$ mm in three-dimensional analysis, where the transverse detonation (TD) propagates from left to right. In front of a cylindrical body, an axial flow induced by the initial disturbance generates the compression waves, which interact each other in front of a cylindrical body, and finally they develop into the transverse detonation. Figure 4 clarifies the wave structure of the transverse detonation in Fig. 3 precisely, using the time evolution of the density contour plots on the plane of the stagnation streamlines in front of the cylindrical body (yellow zone in Fig. 1). The upper-side gray line in each figure indicates the surface of the cylindrical body. The transverse detonation travels from left to right as seen in Fig.3. The wave structure of the transverse detonation looks similar to that of spinning detonation in a circular tube [4]. Maintaining the wave structure, the transverse detonation propagates only in one direction, which is perpendicularly to the flow direction, in front of a cylindrical body. Figure 5 shows the instantaneous density contour plots on the plane of the stagnation streamlines for $L=12$ mm. In this case, two transverse detonations appear. Table 1 shows the relationship between spanwise length of cylinder (L), number of TD (n), distance between two TDs (L_{TD}), width of TD (W_{TD}), strength of TD ($S = p_s / p_1 - 1$: p_s is the peak pressure of midpoint of W_{TD} and p_1 is the pressure in front of TD) and cell width calculated by two-dimensional analysis of the channel C-J detonation in the same gas conditions (λ_{CJ}). The cell width is the mean value of the cell widths of the 2D detonation propagating steadily in a enough wide channel. Figure 6(a) shows the traveling time of TD in L (τ) and propagation velocity of TD (V_{TD}) and L . V_{TD} is almost constant regardless of L , and so τ linearly increases with the increase of L . There is a critical value, that is 10mm, for the number of TD in Table 1. In the case of $L=11, 12$ mm, a new transverse detonation appears in addition to the original transverse detonation. Considering the critical value 10mm, it corresponds to the cell width, which is a characteristic value based on the detonable gas mixture. Therefore n increases when L_{TD} is over λ_{CJ} . Figure 6(b) indicates that the relationship between L_{TD} and L , and we can predict the behavior of the bigger L , that is L_{TD} never exceed λ_{CJ} . In the present simulations, we used the periodic boundary condition in the spanwise direction. This boundary condition implies that the spanwise length is infinite for the one-sided propagating detonation wave, as well as the spinning detonation.

Table 1. The relationship between spanwise length L and computed parameters

Case	spanwise length L (mm)	number of TD n	length of TD L_{TD} (mm)	width of TD W_{TD} (mm)	strength of TD S
(a)	4	1	4	0.51	2.9
(b)	5	1	5	0.52	3.3
(c)	6	1	6	0.53	3.7
(d)	7	1	7	0.55	3.3
(e)	8	1	8	0.58	3.2
(f)	9	1	9	0.61	3.0
(g)	10	1	10	0.65	2.9
(h)	11	2	5.5	0.53	3.3
(i)	12	2	6	0.53	3.7

The cell width of C-J channel detonation: $\lambda_{CJ}=10\text{mm}$

4 Conclusions

Shock-induced combustion around a cylindrical body was numerically investigated using two- and three-dimensional Euler equations with a two-step chemical reaction model. In two-dimensional analysis, the regular regime, the large-disturbance regime and the unsteady state appear as observed around a spherical body. However in three-dimensional analysis, the transverse detonation propagating in the one side of the spanwise direction appears in front of the cylinder for $d=3\text{mm}$, where the regular regime appears in two-dimensional analysis. The transverse detonation propagates, maintaining the wave structure. A series of simulations with various spanwise lengths were carried out to see the behavior of the transverse detonation. When the length of transverse detonation is over a certain value, the number of transverse detonations increases. The critical value is equal to the cell width, which is calculated by two-dimensional analysis of the channel C-J detonation.

References

- [1] Hartmuth F. Lehr, 1972. *Experiment on Shock-Induced Combustion*. Astronautica Acta. Vol. 17, pp589-597.
- [2] Akiko Matsuo and Kozo Fujii, 1995. *Computational Study of Large-Disturbance Oscillations in Unsteady Supersonic Combustion Around Projectiles*. AIAA Journal. Vol. 33. No. 10.
- [3] V. P. Korobeinikov, V. A. Levin, V. V. Markov and G. G. Chernyi, 1972. *Propagation of Blast Waves in a Combustible Gas*, Astronautica Acta, Vol. 17, pp529-537.
- [4] J. H. S. Lee, 2008. *The Detonation Phenomenon*, Cambridge University Press.

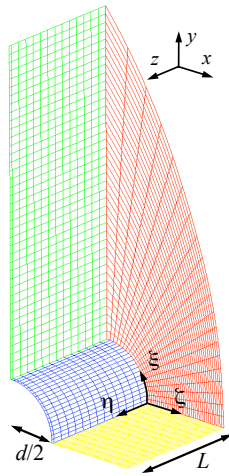


Figure 1. Computational domain (grid points are displayed every 10 points for each direction).

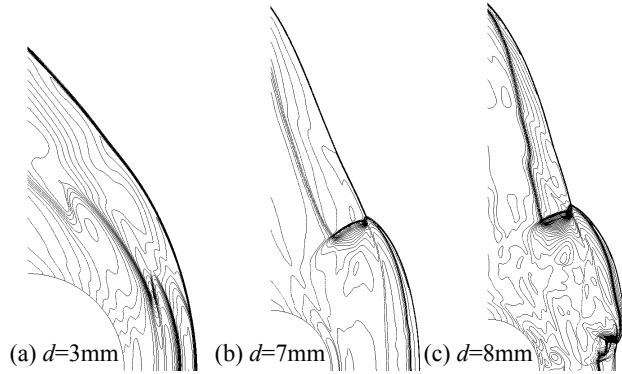


Figure 2. Density contour plots of (a)regular regime, (b)large-disturbance regime and (c)unsteady state in 2D analysis.

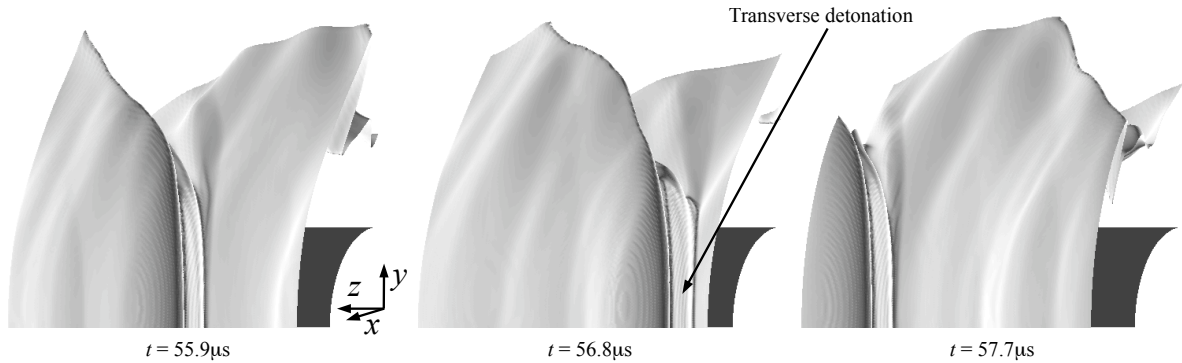


Figure 3. Time evolution of the isosurfaces of the reaction front for $L=5\text{mm}$.

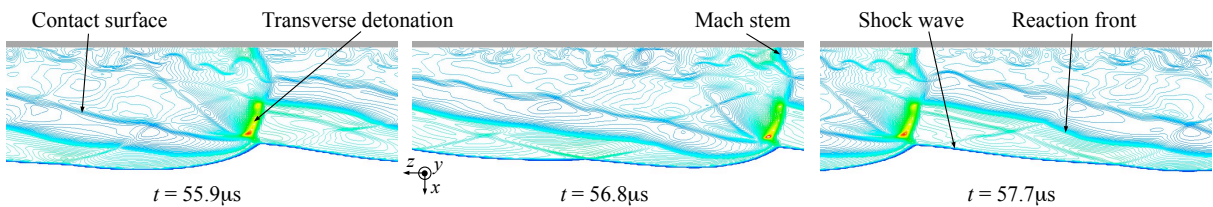


Figure 4. Time evolution of the density contour plots on the plane of the stagnation streamlines for $L=5\text{mm}$.

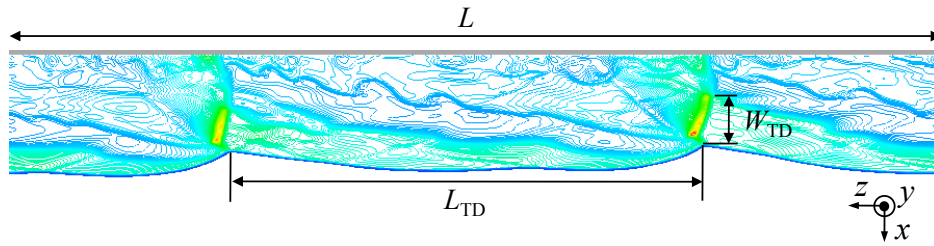


Figure 5. Instantaneous density contour plots on the plane of the stagnation streamlines for $L=12\text{mm}$ ($n=2$).

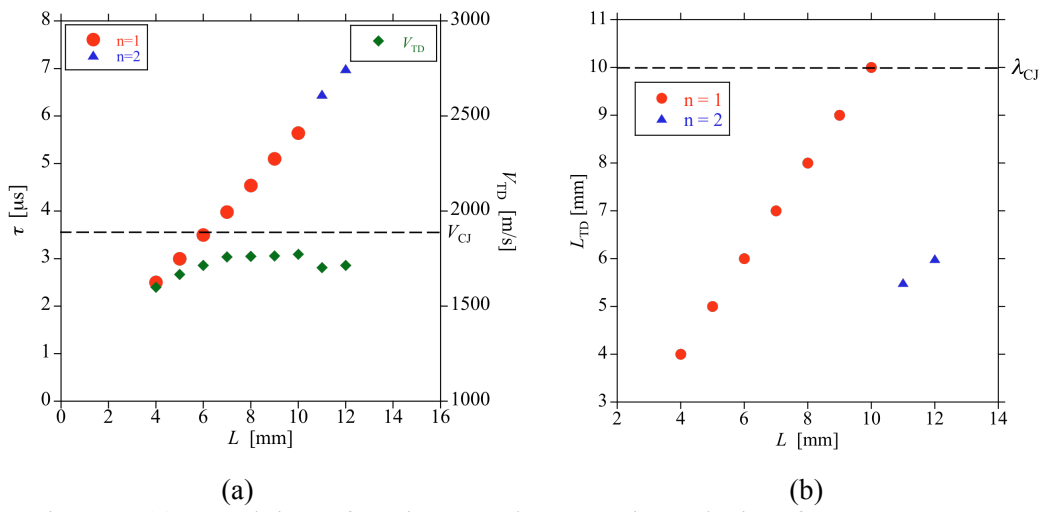


Figure 6. (a) Travel time of TD in $L \tau$ and propagation velocity of TD V_{TD} vs. L .
 (b) Length of TD L_{TD} vs. L .